Backlog-Based Random Access in Wireless Networks: Fluid Limits and Instability Issues

Javad Ghaderi, Sem C. Borst, Phil Whiting

Backlog-Based Random Access in Wireless Networks: Fluid Limits and Instability Issues

Javad Ghaderi[†], Sem Borst[‡], Phil Whiting[‡]
[†]University of Illinois at Urbana-Champaign, [‡]Alcatel-Lucent Bell Labs, Murray Hill

***Abstract*—Backlog-based wireless access schemes are simple and inherently distributed, yet provide a striking capability to match the optimal throughput performance of centralized scheduling mechanisms in a wide range of scenarios. Unfortunately, the type of activation rules for which throughput optimality has been established, may result in excessive backlogs and delays. The use of more aggressive/persistent access schemes than these can improve the delay performance, but does not offer any universal maximum-stability guarantees.**

Motivated by the above issues, we use fluid limits to explore the (in)stability properties of backlog-based random-access algorithms. Such fluid limits have varying qualitative properties, dependent on the specific scenario, ranging from ones with smooth deterministic features, to others which exhibit random oscillatory characteristics. It turns out that more aggressive access schemes continue to provide maximum stability in some networks, e.g. complete interference graphs. As we show however, in other topologies such schemes can drive the system into inefficient states and thus cause instability. Simulation experiments are conducted to illustrate and validate the analytical results.

I. Introduction

Emerging wireless mesh networks typically lack any centralized access control entity, and instead vitally rely on the individual nodes to operate autonomously and to efficiently share the medium in a distributed fashion. This requires the nodes to schedule their individual transmissions and decide on the use of a shared medium based on knowledge that is locally available or only involves limited exchange of information. A popular mechanism for distributed medium access control is provided by the so-called Carrier-Sense Multiple-Access (CSMA) protocol, various incarnations of which are implemented in IEEE 802.11 networks. In the CSMA protocol each node attempts to access the medium after a certain back-off time, but nodes that sense activity of interfering nodes freeze their back-off timer until the medium is sensed idle. Despite their asynchronous and distributed nature, CSMA-like algorithms have been shown to offer the capability of achieving the full capacity region and thus match the optimal throughput performance of centralized scheduling mechanisms operating in slotted time [10]–[12]. More specifically, any throughput vector in the interior of the convex hull associated with the independent sets in the underlying interference graph can be achieved through suitable back-off rates and/or transmission lengths. Based on this observation, various ingenious algorithms have been developed for finding the back-off rates that yield a particular target throughput vector or that optimize a certain concave throughput utility function in scenarios with saturated buffers [10], [11], [15]. In the same spirit, several effective approaches have been devised for adapting the transmission lengths based on backlog information, and been shown to guarantee maximum stability [9], [18], [20].

Roughly speaking, the maximum-stability guarantees were established under the condition that the activity factors of the various nodes behave as logarithmic functions of the backlogs. Unfortunately, such activity factors can induce excessive backlogs and delays, which has triggered a strong interest in developing approaches for improving the delay performance [13], [14], [17], [19]. Motivated by this issue, Ghaderi & Srikant [7] recently showed that it is in fact sufficient for the *logarithms* of the activity factors to behave as logarithmic functions of the backlogs, divided by an arbitrarily slowly increasing, unbounded function. These results indicate that the maximum-stability guarantees are preserved for activity functions that are essentially linear for all practical values of the backlogs, although asymptotically the activity rate must grow slower than any positive power of the backlog.

In the present paper we explore the scope for using more aggressive activity functions in order to improve the delay performance while preserving the maximum-stability guarantees. Since the proof methods of [7], [9], [18] do not easily extend to more aggressive activity functions, we will instead adopt fluid limits where the dynamics of the system are scaled in both space and time. Fluid limits may be interpreted as first-order approximations of the original stochastic process, and provide valuable qualitative insight and a powerful approach for establishing (in)stability properties [2]–[4], [16].

As observed in [1], qualitatively different types of fluid limits can arise, depending on the structure of the interference graph, in conjunction with the functional shape of the activity factors. For sufficiently tame activity functions as in [7], [18], 'fast mixing' is guaranteed, where the activity process evolves on a much faster time scale than the scaled backlogs. Qualitatively similar fluid limits can arise for more aggressive activity functions as well, provided the topology is benign in a certain sense. In different regimes, however, aggressive activity functions can cause 'sluggish mixing', where the activity process evolves on a much slower time scale than the scaled backlogs, yielding oscillatory fluid limits that follow random trajectories. The possible oscillatory behavior of the fluid limit itself does not necessarily imply that the system is unstable, and in some situations maximum stability is in fact maintained. In other scenarios, however, the fluid limit reflects that more aggressive activity functions may force the system into inefficient states for extended periods of time and produce

978-3-901882-45-6/2012 - Copyright is with IFIP

instability.

We will demonstrate instability for super-linear activity functions, but our proof arguments suggest that it can potentially occur for any activity factor that grows as a positive power of the backlog in networks with sufficiently many nodes. In other words, the growth conditions for maximum stability depend on the number of nodes, which seems loosely related to results in [8], [21], [22] characterizing how (upper bounds for) the mean backlog and delay scale as a function of the size of the network.

The remainder of the paper is organized as follows. In Section II, we present a detailed model description. We introduce fluid limits in Section III, and then use these to demonstrate the possible instability of aggressive activity functions in Section IV. Simulation experiments are conducted in Section V to support the analytical results. In Section VI, we make some concluding remarks and identify topics for further research.

II. Model description

We consider a network of several nodes sharing a wireless medium according to a random-access mechanism. The network is represented by an undirected graph $G = (V, E)$ where the set of vertices $V = \{1, \ldots, N\}$ correspond to the various nodes and the set of edges $E \subseteq V \times V$ indicate which pairs of nodes interfere. Nodes that are neighbors in the interference graph are prevented from simultaneous activity, and thus the independent sets correspond to the feasible joint activity states of the network. A node is said to be blocked whenever the node itself or any of its neighbors is active, and unblocked otherwise. Define $S \subseteq \{0,1\}^N$ as the set of feasible joint activity states, i.e., the incidence vectors of all the independent sets of the interference graph, and denote by $\mathcal{C} = \text{conv}(S)$ the capacity region, with $\text{conv}(\cdot)$ indicating the convex hull operator.

Packets arrive at node i as a Poisson process of rate λ_i. The packet transmission times at node i are independent and exponentially distributed with mean $1/\mu_i$. Denote by $\rho_i = \lambda_i/\mu_i$ the load of node i.

Let $U(t) \in S$ represent the joint activity state of the network at time t, with $U_i(t)$ indicating whether node i is active at time t or not. Denote by $Q_i(t)$ the backlog at node i at time t, i.e., the number of packets waiting for transmission or in the process of being transmitted.

As mentioned above, the various nodes share the medium in accordance with a random-access mechanism. When a node ends an activity period (consisting of possibly several back-to-back packet transmissions), it starts a back-off period. The back-off times of node i are independent and exponentially distributed with mean $1/\nu_i$. The back-off period of a node is suspended whenever it becomes blocked by activity of any of its neighbors, and only resumed once the node becomes unblocked again. Thus the back-off period of a node can only end when none of its neighbors are active. Now suppose a back-off period of node i ends at time t. Then the node starts a transmission with probability $\phi_i(Q_i(t))$, with $\phi_i(0) = 0$, and begins the next back-off period otherwise. After the end of a transmission of node i at time t, it releases the medium and begins a back-off period with probability $\psi_i(Q_i(t^-))$, or starts the next transmission otherwise, with $\psi_i(1) = 1$. Equivalently, node i may be thought of as activating at an exponential rate $f_i(Q_i(t))$, with $f_i(\cdot) = \nu_i\phi_i(\cdot)$, whenever it is unblocked at time t, and de-activating at rate $g_i(Q_i(t))$, with $g_i(\cdot) = \mu_i\psi_i(\cdot)$, whenever it is active at time t. For conciseness, the functions $f_i(\cdot)$ and $g_i(\cdot)$ will be referred to as activation and de-activation functions, respectively.

There are two special cases worth mentioning that (loosely) correspond to random-access schemes considered in the literature before. First of all, in case $\phi_i(Q_i) = 1$ for all $Q_i \geq 1$ and $\psi_i(Q_i) = 0$ for all $Q_i \geq 2$, node i starts a transmission each time a back-off period ends, and does not release the medium, i.e., continues transmitting until its entire backlog has been cleared. This corresponds to the random-capture scheme considered in [5]. In case $\mu_i = 1$, $\nu_i = 1$, $\phi_i(Q_i) = 1 - \psi_i(Q_i)$, and $\psi_i(Q_i) = 1/(1 + r_i(Q_i))$, node i may be thought of as becoming (or continuing to be) active with probability $r_i(Q_i(t))/(1 + r_i(Q_i(t)))$ each time a unit-rate Poisson clock ticks. This roughly corresponds to the scheme considered in [7], [9], [18] based on Glauber dynamics with a 'weight' function $w_i(Q_i) = \log(r_i(Q_i))$, except that the latter scheme operates with a random round-robin clock, and uses $\tilde{w}_i(Q_i) = \max\{w_i(Q_i), \frac{\epsilon}{2N} w_i(Q_{\max})\}$, with $Q_{\max} = \max_{j=1,\ldots,N} Q_j$.

Under the above-described backlog-based schemes, the process $\{(U(t), Q(t))\}_{t\geq 0}$ evolves as a continuous-time Markov process with state space $S \times \mathbb{N}^N$. Transitions (due to arrivals) from a state (U, Q) to $(U, Q + e_i)$ occur at rate λ_i, transitions (due to activations) from a state (U, Q) with $Q_i \geq 1$, $U_i = 0$, and $U_j = 0$ for all neighbors of node i, to $(U + e_i, Q)$ occur at rate $\nu_i f_i(Q_i)$, transitions (due to transmission completions followed back-to-back by a subsequent transmission) from a state (U, Q) with $U_i = 1$ (and thus $Q_i \geq 1$) to $(U, Q - e_i)$ occur at rate $\mu_i(1 - g_i(Q_i))$, transitions (due to transmission completions followed by a back-off period) from a state (U, Q) with $U_i = 1$ (and thus $Q_i \geq 1$) to $(U - e_i, Q - e_i)$ occur at rate $\mu_i g_i(Q_i)$.

We are interested to determine under what conditions the system is stable, i.e., the Markov process $\{(U(t), Q(t))\}_{t\geq 0}$ is positive-recurrent. It is easily seen that $(\rho_1, \ldots, \rho_N) < \sigma \in \mathcal{C}$ is a necessary condition for that to be the case. In [7], it is shown that this condition is in fact also sufficient for $f \equiv 1$ and $g(Q_i) = (1 + r_i(Q_i))^{-1}$, for functions of the form $r_i(Q_i) = \exp(\log(Q_i)/y_i(Q_i))$, where $y_i(Q_i)$ is allowed to increase to infinity at an arbitrarily slow rate. For practical purposes, this means that the function $r_i(Q_i)$ is essentially allowed to be linear, except that it must eventually grow to infinity slower than any positive power of Q_i. Results in [1] suggest that more aggressive choices of the functions $f_i(\cdot)$ and $g_i(\cdot)$, which translate into functions $r_i(\cdot)$ that grow faster to infinity, can improve the delay performance. In view of these results, we will be particularly interested in such functions

$r_i(\cdot)$, where the sufficient stability conditions of [7] are *not* fulfilled. In order to examine under what conditions the system will remain stable then, we examine fluid limits as introduced in the next section.

III. Fluid limits

In order to obtain fluid limits, the original stochastic process is scaled in both space and time. More specifically, we consider a sequence of processes $\{(U^R(t), Q^R(t))\}_{t\geq 0}$ indexed by a sequence of positive integers R, each governed by similar statistical laws as the original process, where the initial states satisfy $\sum_{i=1}^N Q_i^R(0) = R$ and $Q_i^R(0)/R \to q_i$ as $R \to \infty$. The process $\{(U^R(Rt), \frac{1}{R}Q^R(Rt))\}_{t\geq 0}$ is referred to as the fluid-scaled version of the process $\{(U^R(t), Q^R(t)\}_{t\geq 0}$. Any (possibly random) weak limit $\{q(t)\}_{t\geq 0}$ of the sequence $\{\frac{1}{R}Q^R(Rt)\}_{t\geq 0}$, as $R \to \infty$, is called a fluid limit.

In the next section we will use fluid limits to demonstrate the possible instability of 'aggressive' activation and/or de-activation functions. In order to show that such aggressive functions do not imply instability in all topologies, we first examine a complete K-partite graph as considered in [5], where the nodes can be partitioned into $K \geq 2$ components. All nodes are connected except those belonging to the same component. Denote by $M_k \subseteq \{1, \ldots, N\}$ the subset of nodes belonging the k-th component. Once one of the nodes in component M_k is active, other nodes within M_k can become active as well, but none of the nodes in the other components M_l, $l \neq k$, can be active. The necessary stability condition then takes the form $\rho = \sum_{k=1}^K \hat{\rho}_k < 1$, with $\hat{\rho}_k = \max_{i\in M_k} \rho_i$ denoting the maximum traffic intensity of any of the nodes in the k-th component.

Now consider the case that each node operates with an activation function $f(x) \equiv 1$, $x \geq 1$ and a de-activation function $g(x) = \mathrm{o}(x^{-\gamma})$, with $\gamma > 1$, which subsumes the random-capture scheme with $g(x) \equiv 0$ for all $x \geq 1$ in [5]. Since the de-activation rate decays so sharply, the probability of a node releasing the medium once it has started transmitting with an initial backlog of order R, is vanishingly small, until the backlog falls below order R or the total number of transmissions exceeds order R (but the latter implies the former). Hence, in the fluid limit, a node must completely empty almost surely before it releases the medium. Because of the interference constraints, it further follows that once the activity process enters one of the components, it remains there until all the queues in that component have entirely drained. For conciseness, the system is said to be in an M_k-period during time intervals when the activity process resides in component M_k.

Based on the above informal observations, we now proceed with a more detailed description of the fluid limit process.

Assume that the system enters an M_k-period at time t, then

(a) It spends a time period $T_k(t) = \max_{i\in M_k} \frac{q_i(t)}{\mu_i - \lambda_i}$ in M_k.
(b) During this period, the queues of the nodes in M_k drain at a linear rate (or remain zero)

$$q_i(t+u) = \max\{q_i(t) + (\lambda_i - \mu_i)u, 0\}, \ \forall i \in M_k$$

while the queues of the other nodes fill at a linear rate

$$q_i(t+u) = q_i(t) + \lambda_i u, \ \forall i \notin M_k,$$

for all $u \in [0, T_k(t)]$.

(c) At time $t + T_k(t)$, the system switches to schedule M_l, $l \neq k$, with probability

$$p_{kl}(t+T_k(t)) = \lim_{R\to\infty} \frac{\sum_{i\in M_k} f(Rq_i(t+T_k(t)))}{\sum_{l'\neq k}\sum_{i\in M_{l'}} f(Rq_i(t+T_k(t)))}.$$

Thus the fluid limit follows piece-wise linear sample paths (almost surely), with switches between different periods governed by the transition probabilities specified above.

Now define the Lyapunov function $L(t) := \sum_{k=1}^K \hat{q}_k(t)$, with $\hat{q}_k(t) = \max_{i\in M_k} q_i(t)/\mu_i$. Then, $\frac{d}{dt}L(t) \leq \sum_{k=1}^K \hat{\rho}_k - 1 = \rho - 1 < 0$ almost everywhere when $\rho < 1$, as long as $L(t) > 0$. Therefore, $L(t) = 0$, and hence $q(t) = 0$, for all $t \geq T$, with $T = \frac{L(0)}{1-\rho} < \infty$, implying stability [2], [4], even though the fluid limit behavior is not smooth at all.

We now turn to a 'nearly' complete 3-partite graph with two nodes in each component as shown in Figure 1(a) as a prototypical network where aggressive functions can cause instability. The intuitive explanation for the potential instability may be described as follows. Denote $\rho_0 = \max\{\rho_1, \rho_2\}$, and assume $\rho_3 > \rho_4$ and $\rho_5 < \rho_6$. The fraction of time that at least one of the nodes 1, 2, 3 and 6 is served, must be no less than $\rho = \rho_0 + \rho_3 + \rho_6$ in order for these nodes to be stable. During some of these periods nodes 4 or 5 may also be served, but not simultaneously, i.e., schedule M_4 cannot be used. In other words, the system cannot be stable if schedule M_4 is used for a fraction of the time larger than $1 - \rho$. As it turns out, however, when the de-activation function is sufficiently aggressive, e.g., $g(\cdot) = \mathrm{o}(x^{-\gamma})$, with $\gamma > 1$, schedule M_4 is in fact persistently used for a fraction of the time that does not tend to 0 as ρ approaches 1, which forces the system to be unstable.

Although the above arguments indicate that invoking schedule M_4 is a recipe for trouble, the reason may not be directly evident from the system dynamics, since no obvious inefficiency occurs as long as the queues of nodes 4 and 5 are non-empty. However, the fact that the Lyapunov function $L(t) = \sum_{k=1}^3 \hat{q}_k(t)$ may increase while serving nodes 4 and 5, when $q_3(t) \geq q_4(t)$ and $q_5(t) \leq q_6(t)$, is already highly suggestive. Indeed, serving nodes 4 and 5 may make their queues smaller than those of nodes 3 and 6, leaving these queues to be served by themselves at a later stage, at which point inefficiency inevitably occurs. It is intuitively plausible that such events occur repeatedly with positive probability, but a rigorous proof that this leads to instability is far from simple. Such a proof requires detailed analysis of the underlying stochastic process (in our case via fluid limits), and its conclusion crucially depends on the de-activation function. Indeed, the stability results in [7], [9], [18] indirectly indicate that our network is *not* rendered unstable for sufficiently cautious de-activation functions.

We now characterize the dynamics of the fluid limit process. For an activation function $f(x) \equiv 1$, $x \geq 1$, and a de-

activation function $g(x) = o(x^{-\gamma})$, with $\gamma > 1$, the fluid limit process follows oscillatory piece-wise linear trajectories (almost surely), with random switches, just like for complete partite graphs, and as illustrated in Figure 1(b). In particular, in the fluid limit a node must completely empty almost surely before it releases the medium. Thus, a transition from one component to another occurs when one or both queues in that component hit zero.

We now provide a detailed description of the dynamics of the fluid limit process. Just like for the complete partite graphs, the system is said to be in an M_k-period during the time intervals when the activity process resides in component M_k. For notational convenience, we henceforth assume $\mu_i \equiv 1$, so that $\rho_i \equiv \lambda_i$, for all $i = 1, \ldots, N$. The justification for the description as presented below follows from a collection of lemmas and propositions which are stated and proved in [6].

1) M_1-period: Assume the system enters an M_1-period at time t, then

(a) It spends a time period $T_1(t) = \max\left\{\frac{q_1(t)}{1-\rho_1}, \frac{q_2(t)}{1-\rho_2}\right\}$ in M_1.

(b) During this period, the queues of nodes 1 and 2 drain at a linear rate (or remain zero)

$$q_i(t+u) = \max\{q_i(t) - (1-\rho_i)u, 0\}, \text{ for } i = 1, 2,$$

while the queues of nodes 3, 4, 5, 6 fill at a linear rate

$$q_i(t+u) = q_i(t) + \rho_i u, \text{ for } i = 3, 4, 5, 6,$$

for all $u \in [0, T_1(t)]$. In particular, $q_1(t + T_1(t)) = q_2(t + T_1(t)) = 0$.

(c) At time $t + T_1(t)$, the system switches to one of the schedules M_2, M_3 or M_4 with the following transition probabilities

$$p_{12}(t + T_1(t)) = \lim_{R\to\infty} \frac{1}{F}\left(f_3 + f_4\frac{f_3}{f_3+f_5}\right)$$
$$p_{13}(t + T_1(t)) = \lim_{R\to\infty} \frac{1}{F}\left(f_6 + f_5\frac{f_6}{f_4+f_6}\right)$$
$$p_{14}(t + T_1(t)) = \lim_{R\to\infty} \frac{1}{F}\left(f_4\frac{f_5}{f_3+f_5} + f_5\frac{f_4}{f_4+f_6}\right)$$

with $F = f_3+f_4+f_5+f_6$, and $f_j = f(Rq_j(t+T_1(t)))$, $j = 3, 4, 5, 6$. Note that in case $f_i(x) = 1$, $x \geq 1$, the above transition probabilities are simply given by $p_{12} = \frac{3}{8}$, $p_{13} = \frac{3}{8}$, $p_{14} = \frac{1}{4}$.

2) M_2-period: Assume that the system enters an M_2-period at time t, then

(a) The system spends a time period $T_2(t) = \frac{q_3(t)}{1-\rho_3}$ in M_2.

(b) During this period, the queues of nodes 3 and 4 drain (or remain zero)

$$q_i(t+u) = \max\{q_i(t) - (1-\rho_i)u, 0\}, \text{ for } i = 3, 4,$$

while the queues of nodes 1, 2, 5, 6 fill at a linear rate

$$q_i(t+u) = q_i(t) + \rho_i u, \text{ for } i = 1, 2, 5, 6,$$

for all $u \in [0, T_2(t)]$. In particular, $q_3(t + T_2(t)) = 0$.

(c) At time $t + T_2(t)$, the system switches to one of the schedules M_1, M_3 or M_4. In order to determine which of these events can occur, we need to distinguish between three cases, depending on whether $\frac{q_3(t)}{1-\rho_3}$ is (i) larger than, (ii) equal to, or (iii) smaller than $\frac{q_4(t)}{1-\rho_4}$.

In case (i), i.e., $\frac{q_3(t)}{1-\rho_3} > \frac{q_4(t)}{1-\rho_4}$, the queue of node 4 has emptied before time $t + T_2(t)$, and remained empty (on the fluid scale) since then, precluding a switch to schedule M_4 (except for a negligible duration on the fluid scale), only allowing the system to switch to either schedule M_1 or M_3. The corresponding transition probabilities are difficult to obtain in explicit form. Note that in order for any of the nodes 1, 2, 5 or 6 to activate, node 3 must be inactive. In order for nodes 1, 2 or 6 to activate, node 4 must be inactive as well, but the latter is not necessary in order for node 5 to activate. Since node 4 may be active even when it is empty on the fluid scale, it follows that node 5 enjoys an advantage in competing for access to the medium over nodes 1, 2 and 6. While it may be argued that node 4 is active with probability ρ_4 by the time node 3 becomes inactive for the first time, the resulting probabilities for the various nodes to gain access to the medium first do not seem to allow a simple expression.

In case (ii), i.e., $\frac{q_3(t)}{1-\rho_3} = \frac{q_4(t)}{1-\rho_4}$, the queues of nodes 3 and 4 both empty at time $T_2(t)$, barring once again a switch to schedule M_4, and permitting only a switch to either schedule M_1 or M_3. Just like in the previous case, node 5 is the only one able to activate during periods where node 3 is inactive while node 4 is active, and hence enjoys an advantage in competing for access to the medium. In fact, node 5 will gain access to the medium first almost surely if node 3 is the first one to become inactive (in the pre-limit). The probability of that event, and hence the transition probabilities to M_1 and M_3, depends on queue length differences between nodes 3 and 4 at time t that are affected by the history of the process and are not visible on the fluid scale.

In case (iii), i.e., $\frac{q_3(t)}{1-\rho_3} < \frac{q_4(t)}{1-\rho_4}$, the queue of node 4 is still non-empty by time $t + T_2(t)$, forcing a switch to schedule M_4 with probability 1.

3) M_3-period: The dynamics for an M_3-period are entirely symmetric to those for an M_2-period, but will be replicated below for completeness.

Assume that the system enters an M_3-period at time t, then

(a) The system spends a time period $T_3(t) = \frac{q_6(t)}{1-\rho_6}$ in M_3.

(b) During this period, the queues of nodes 5 and 6 drain (or remain zero)

$$q_i(t+u) = \max\{q_i(t) - (1-\rho_i)u, 0\}, \text{ for } i = 5, 6,$$

while the queues of nodes 1, 2, 3, 4 fill at a linear rate

$$q_i(t+u) = q_i(t) + \rho_i u, \text{ for } i = 1, 2, 3, 4,$$

for all $u \in [0, T_3(t)]$. In particular, $q_6(t + T_3(t)) = 0$.

(c) At time $t + T_3(t)$, the system switches to one of the schedules M_1, M_2 or M_4. In order to determine which of these events can occur, we need to distinguish between three cases, depending on whether $\frac{q_5(t)}{1-\rho_5}$ is (i) smaller than, (ii) equal to, or (iii) larger than $\frac{q_6(t)}{1-\rho_6}$.
In case (i), i.e., $\frac{q_5(t)}{1-\rho_5} < \frac{q_6(t)}{1-\rho_6}$, the queue of node 5 has emptied before time $t + T_3(t)$, and remained empty (on the fluid scale) since then, precluding a switch to schedule M_4 (except for a negligible period on the fluid scale), only allowing the system to switch to either schedule M_1 or M_2. The corresponding transition probabilities are difficult to obtain in explicit form for similar reasons as mentioned in case 2(c)(i).
In case (ii), i.e., $\frac{q_5(t)}{1-\rho_5} = \frac{q_6(t)}{1-\rho_6}$, the queues of nodes 5 and 6 both empty at time $T_3(t)$, barring once again a switch to schedule M_4, and allowing only a switch to either schedule M_1 or M_2. For similar reasons as mentioned in case 2(c)(ii), the corresponding transition probabilities depend on queue length differences that are affected by the history of the process and are not visible on the fluid scale.
In case (iii), i.e., $\frac{q_5(t)}{1-\rho_5} > \frac{q_6(t)}{1-\rho_6}$, the queue of node 5 is still non-empty by time $t + T_3(t)$, forcing a switch to schedule M_4 with probability 1.

4) M_4-period: Assume that the system enters an M_4-period at time t, then

(a) It spends a time period $T_4(t) = \min\left\{\frac{q_4(t)}{1-\rho_4}, \frac{q_5(t)}{1-\rho_5}\right\}$ in M_4.

(b) During this period, the queues of nodes 4 and 5 drain at a linear rate

$$q_i(t+u) = q_i(t) - (1-\rho_i)u, \text{ for } i = 4, 5,$$

while the queues of nodes 1, 2, 3, 6 fill at a linear rate

$$q_i(t+u) = q_i(t) + \rho_i u, \text{ for } i = 1, 2, 3, 6,$$

$u \in [0, T_4(t)]$. In particular, $\min\{q_4(t + T_4(t)), q_5(t + T_4(t))\} = 0$.

(c) At time $t+T_4(t)$, the system switches to either schedule M_2 or M_3. In order to determine which of these events can occur, we need to distinguish between three cases, depending on whether $\frac{q_4(t)}{1-\rho_4}$ is (i) larger than, (ii) equal to, or (iii) smaller than $\frac{q_5(t)}{1-\rho_5}$.
In case (i), i.e., $\frac{q_4(t)}{1-\rho_4} > \frac{q_5(t)}{1-\rho_5}$, we have $q_4(t+T_4(t)) > 0$, i.e., the queue of node 4 is still non-empty by time $t + T_4(t)$, causing a switch to schedule M_2 with probability 1.
In case (ii), i.e., $\frac{q_4(t)}{1-\rho_4} = \frac{q_5(t)}{1-\rho_5}$, we have $q_4(t+T_4(t)) = q_5(t + T_4(t)) = 0$, i.e., the queues of nodes 4 and 5 both empty at time $t + T_4(t)$. Even though both queues empty at the same time on the fluid scale, there will with overwhelming probability be a long period in the pre-limit where one of the nodes has become inactive for the first time while the other one has yet to do so. Since both nodes 4 and 5 must be inactive in order for nodes 1 and 2 to activate, these nodes have no chance to activate during that period, but either node 3 or node 6 does, depending on whether node 5 or node 4 is the first one to become inactive. As a result, the system cannot switch to schedule M_1, but only to M_2 or M_3. In fact, a switch to M_2 will occur almost surely if node 5 is the first one to become inactive, while a switch to M_3 will occur almost surely if node 4 is the first one to become inactive. The probabilities of these two scenarios, and hence the transition probabilities to M_2 and M_3, depend on queue length differences between nodes 4 and 5 at time t that are affected by the history of the process and are not visible on the fluid scale.
In case (iii), i.e., $\frac{q_4(t)}{1-\rho_4} < \frac{q_5(t)}{1-\rho_5}$, we have $q_5(t+T_4(t)) > 0$, i.e., the queue of node 5 is still non-empty by time $t + T_4(t)$, forcing a switch to schedule M_3 with probability 1.

Remark 1: As noted in the above description of the fluid limit process, in cases 2(c)(ii), 3(c)(ii) and 4(c)(ii) the transition probabilities from an M_2-period to an M_1 or M_3-period, from an M_3-period to an M_1 or M_2-period, and from an M_4 to an M_2 or M_3-period, depend on queue length differences that are affected by the history of the process and are not visible on the fluid scale. Depending on whether or not the initial state and parameter values allow for these cases to arise, the resulting fluid limit process may thus be non-Markovian, even though the original stochastic process is Markovian.

Remark 2: It is worth observing that when $q_3(t) = 0$, $q_4(t) > 0$, $q_5(t) = 0$, the above description of the fluid limit process yields an indefinite alternation between zero-length M_2- and M_4-periods. The way the fluid limit process then actually evolves, is that for a period of time $q_4(t)/(1-\rho_4)$, the queue of node 4 drains at a rate $1-\rho_4$, the queues of nodes 3 and 5 remain at zero, and the queues of nodes 1, 2, and 6 fill at rates ρ_1, ρ_2 and ρ_6, respectively. This evolution reflects that in the original stochastic process nodes 3 and 5 take turns in accessing the medium, without their queues ever growing significantly, while node 4 holds on to the medium continuously and gradually drains its queue. At the end of such a time period, which we will refer to as an M_{2+4}-period, the system switches to either schedule M_1 or M_3. As we will see later, an M_{2+4}-period can occur at most once, and never arise again after some finite time, and hence we will not consider these periods in further detail. Similar comments apply when $q_4(t) = 0$, $q_5(t) > 0$, $q_6(t) = 0$, producing a succession of zero-length M_3- and M_4-periods.

IV. Instability results

We now use the characterization of the fluid limit process presented in the previous section to prove instability. In order to do so, we adopt the Lyapunov function $L(t) = \sum_{k=1}^{3} \hat{q}_k(t)$, and will show that the load $L(t)$ grows without bound almost surely. Note that the load $L(t)$ increases during M_4-periods when the system is in a natural state, i.e., $q_3(t) \geq q_4(t)$ and $q_5(t) \leq q_6(t)$. As mentioned above, a natural state is reached in finite time. In order to prove that the load $L(t)$

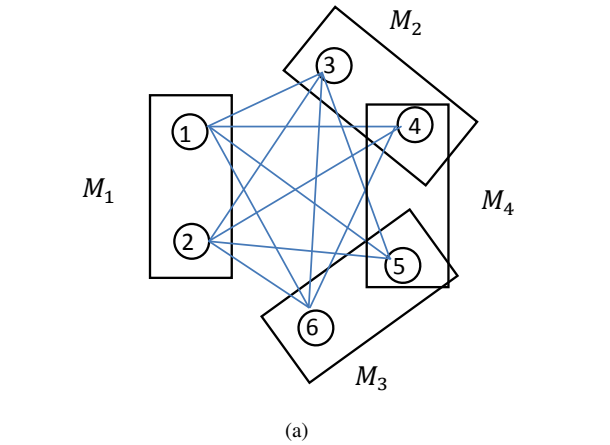

(a)

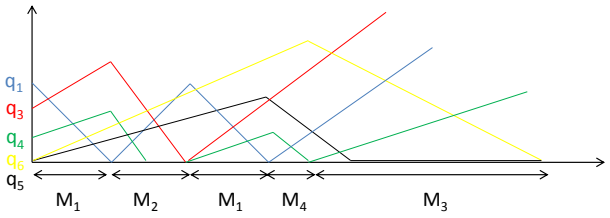

(b)

Fig. 1. (a) A network with 4 possible schedules obtained by removing 1 edge from a 3-partite complete network. (b) A fluid sample path corresponding to the sequence $M_1 \to M_2 \to M_1 \to M_4 \to M_3$.

grows without bound, it thus remains to be established that M_4-periods occur for substantial periods of time.

In preparation for the instability proof, we first state two auxiliary lemmas. It will be convenient to view the evolution of the fluid limit process, and in particular the Lyapunov function $L(t)$, over the course of cycles. The i-th cycle is the period from the start of the $(i-1)$-th M_1-period to the start of the i-th M_1 period. Denote by t_i the start time of the i-th cycle. It is easily seen that there must be an infinite number of cycles (and if there were only a finite number, one of the nodes would never be served again after some finite time, the fluid limit process is unstable regardless).

The next lemma shows that the duration of a cycle and the possible increase in the load over the course of a cycle are linearly bounded in the load at the start of the cycle.

Lemma 1: The duration of the i-th cycle, $\Delta T_i = t_{i+1} - t_i$, and the increase in the load over the course of the i-th cycle, $\Delta L_i = L(t_{i+1}) - L(t_i) = L(t_i + \Delta T_i) - L(t_i)$, are bounded from above by

$$\Delta T_i \le C_T L(t_i) \text{ and } \Delta L_i \le C_L L(t_i)$$

for all $\rho \le 1$, where $C_T = \frac{1}{1-\rho_3-\rho_6}\left(\frac{1}{1-\rho_2} + \frac{1}{1-\max\{\rho_4,\rho_5\}}\right)$ and $C_L = \frac{\rho_3+\rho_6}{1-\max\{\rho_4,\rho_5\}}$.

In order to establish that the durations of M_4-periods are non-negligible, it will be useful to introduce the notion of 'weakly-balanced' queues, ensuring that the queues of nodes 4 and 5 are not too small compared to the queues of nodes 3 and 6.

Definition 1: Let $\beta^{\min}$ and $\beta^{\max}$ be fixed positive constants. The queues are said to be weakly-balanced in a given cycle (with respect to $\beta^{\min}$ and $\beta^{\max}$) if $\beta^{\min} \le \frac{q_3(t)}{q_5(t)}, \frac{q_6(t)}{q_4(t)} \le \beta^{\max}$, with t denoting the time when the M_1-period ends that initiated the cycle.

The next lemma shows that over two consecutive cycles, the queues will be weakly-balanced with probability at least 1/3.

Lemma 2: Let

$$\epsilon = \frac{\rho_2}{2\left(\rho_2 + (\rho_3+\rho_6)\frac{1-\min\{\rho_4,\rho_5\}}{1-\max\{\rho_4,\rho_5\}}\right)} \ge \frac{\rho_2}{\rho}\frac{1-\max\{\rho_4,\rho_5\}}{1-\min\{\rho_4,\rho_5\}}.$$

Then over two consecutive cycles, with probability at least 1/3, the queues will be weakly-balanced in at least one of these cycles with

$$\beta^{\max} = \frac{\max\{\rho_3,\rho_6\} + (1-\rho_2)(1-\epsilon)/\epsilon}{\min\{\rho_4,\rho_5\}}$$

and $\beta^{\min} = \frac{1}{\beta^{\max}}$.

As suggested by the above lemma, it will be convenient to consider pairs of two consecutive cycles in order to prove instability of the fluid limit process. Denote $i_0 = \min\{i = 1,2,\cdots : q_3(t_i) \ge q_4(t_i), q_5(t_i) \le q_6(t_i)\}$, with t_i denoting the start time of the i-th cycle as before. As noted earlier $q_3(t) \ge q_4(t)$ and $q_5(t) \le q_6(t)$ for all $t \ge T^{(0)} = \max\{q_4(0) - q_3(0), q_5(0) - q_6(0), 0\}/\delta$ and $q(T) \ne 0$, hence i_0 is well-defined and $t_{i_0} \le T^{(0)} \le L(0)/\delta$.

Let D_k be the pair of cycles consisting of cycles i_0+2k-2 and i_0+2k-1, $k = 1,2,\ldots$. With minor abuse of notation, denote by $T_k = t_{i_0+2k-2}$ the start time of D_k and $L_k = L(T_k)$. Denote by $\Delta T_k = T_{k+1} - T_k$ the duration of D_k and by $\Delta L_k = L_{k+1} - L_k$ the increase in $L(t)$ over the course of D_k.

The next proposition shows that for ρ sufficiently close to 1 the load cannot significantly decrease over a pair of cycles and will increase by a substantial amount with non-zero-probability. We henceforth assume $(\rho_1,\rho_2,\rho_3,\rho_4,\rho_5,\rho_6) = \rho(\kappa_1,\kappa_2,\kappa_3,\kappa_3-\alpha,\kappa_6-\alpha,\kappa_6)$ with $\max\{\kappa_1,\kappa_2\}+\kappa_3+\kappa_6 = 1$ and $\alpha < \min\{\kappa_3,\kappa_6\}$.

Proposition 1: Let $C = C_T(2+C_L)$, with C_T and C_L as specified in Lemma 1, $\theta = 1-(1-\rho)C$, $p = 1/12$. Over cycle pairs D_k, $k = 1,2,\ldots,$

(i) $\Delta T_k \le C L_k$;
(ii) $L(t) \ge \theta L_k$ for all $t \in [T_k, T_{k+1}]$;
(iii) $\mathbb{P}\big(L_{k+1} - \theta L_k \ge \delta(\rho)\theta L_k | L_k\big) \ge p$,

with $\delta(\rho)$ a constant, depending on ρ, and $\delta(\rho) \uparrow \delta = \frac{1}{\beta^{\max}(1+\beta^{\max})(1+\alpha-\min\{\kappa_3,\kappa_6\})}$, as $\rho \uparrow 1$.

Proof:

We first show part (i). Using Lemma 2, we find

$$\begin{aligned}\Delta T_k &= \Delta T_{i_0+2k-2} + \Delta T_{i_0+2k-1} \\ &\le C_T(L(T_{i_0+2k-2}) + L(T_{i_0+2k-1})) \le C_T(2+C_L)L_k.\end{aligned}$$

In order to prove part (ii), note that $L(t)$ cannot decrease at a larger rate than $1-\rho$, so that in view of part (i),

$$\begin{aligned} L_t &\geq L_k - (1-\rho)(t-T_k) \\ &\geq L_k - (1-\rho)\Delta T_k \\ &\geq (1-(1-\rho)C)L_k \\ &= \theta L_k \end{aligned}$$

for all $t \in [T_k, T_{k+1}]$.

We now turn to part (iii). Suppose that the following event occurs: the queues are weakly-balanced at the end of an M_1-period, say time τ, during D_k (which according to Lemma 2) happens with at least probability 1/3) and the system then enters an M_4-period (which happens with probability 1/4). Recalling that $\rho_3 \geq \rho_4$, $q_3(t) \geq q_4(t)$, $\rho_5 \leq \rho_6$ and $q_5(t) \leq q_6(t)$, we find that during the M_4-period $L(t)$ increases by

$$\rho \min\left\{\frac{q_4(\tau)}{1-\rho_4}, \frac{q_5(\tau)}{1-\rho_5}\right\} \geq \rho \frac{\min\{q_4(\tau), q_5(\tau)\}}{1-\rho\min\{\kappa_3,\kappa_6\}+\rho\alpha}.$$

Since the queues are weakly-balanced, we deduce $q_3(\tau) \leq \beta^{\max} q_5(\tau) \leq \beta^{\max} q_6(\tau) \leq (\beta^{\max})^2 q_4(\tau)$ and $q_6(\tau) \leq \beta^{\max} q_4(\tau) \leq \beta^{\max} q_3(\tau) \leq (\beta^{\max})^2 q_5(\tau)$. Noting that $q_1(\tau) = q_2(\tau) = 0$, we obtain

$$L(\tau) = q_3(\tau)+q_6(\tau) \leq (1+\beta^{\max})q_6(\tau) \leq \beta^{\max}(1+\beta^{\max})q_4(\tau),$$

and also

$$L(\tau) = q_3(\tau)+q_6(\tau) \leq (1+\beta^{\max})q_3(\tau) \leq \beta^{\max}(1+\beta^{\max})q_5(\tau).$$

So

$$L(\tau) \leq \beta^{\max}(1+\beta^{\max})\min\{q_4(\tau), q_5(\tau)\},$$

and thus the increase in $L(t)$ during the M_4-period is no less than $\delta(\rho)L(\tau)$, with

$$\delta(\rho) = \frac{\rho}{\beta^{\max}(1+\beta^{\max})(1-\rho\min\{\kappa_3,\kappa_6\}+\rho\alpha)}.$$

Using part (i) once again, we conclude that with at least probability 1/12,

$$\begin{aligned} L_{k+1} &\geq L_k + \delta(\rho)L(\tau) - (1-\rho)\Delta T_k \\ &\geq L_k + \delta(\rho)(L_k - (1-\rho)\Delta T_k) - (1-\rho)\Delta T_k \\ &= (1+\delta(\rho))(L_k - (1-\rho)\Delta T_k) \\ &\geq (1+\delta(\rho))(L_k - (1-\rho)CL_k) \\ &= (1+\delta(\rho))\theta L_k. \end{aligned}$$

■

Armed with the above proposition, we now proceed to prove that the fluid limit process is unstable, in the sense that $L(T) \to \infty$ as $T \to \infty$. In fact, $L(T)$ grows faster than any sub-linear function $T^{\frac{1}{m}}$, $m > 1$, as stated in the next theorem. Let $(\rho_1, \rho_2, \rho_3, \rho_4, \rho_5, \rho_6) = \rho\kappa$, where $\kappa = (\kappa_1, \kappa_2, \kappa_3, \kappa_4, \kappa_5, \kappa_6)$ with $\max\{\kappa_1, \kappa_2\} + \kappa_3 + \kappa_6 = 1$ and $\kappa_3 > \kappa_4$ and $\kappa_5 < \kappa_6$. The fluid limit process can then be shown to be unstable in the sense that $L(T) = \sum_{k=1}^{3} \max_{i \in M_k} q_i(t) \to \infty$ as $T \to \infty$, as stated in the next theorem.

Theorem 1: Consider the network of Figure 1(a), and suppose $f_i(x) \equiv 1$, $x \geq 1$, and $g_i(x) = \mathrm{o}(x^{-\gamma})$, with $\gamma > 1$. For any $m > 1$, there exists a constant $\rho^* = \rho^*(\kappa, m) < 1$, such that for all $\rho \in (\rho^*, 1]$,

$$\limsup_{T\to\infty} \mathbb{E}\left\{\frac{T}{L^m(T)}\right\} = 0,$$

for any initial state $q(0)$ with $|L(0)| = 1$.

Corollary 1: For any $m > 1$, there exists a constant $\rho^* = \rho^*(\kappa, m) < 1$, such that for all $\rho \in (\rho^*, 1]$,

$$\liminf_{T\to\infty} \frac{L(T)}{T^{1/m}} = \infty,$$

almost surely.

The original stochastic process is said to be unstable when $\{(U(t), Q(t))\}_{t\geq 0}$ is transient, and $\|Q(t)\| \to \infty$ almost surely for any initial state $Q(0)$. Exploiting similar arguments as in Meyn [16], the instability of the original stochastic process can be deduced from the instability of the fluid limit process, as stated in the next theorem.

Theorem 2: Consider the network of Figure 1(a), and suppose $f_i(x) \equiv 1$, $x \geq 1$, and $g_i(x) = \mathrm{o}(x^{-\gamma})$, with $\gamma > 1$. Then there exists a constant $\rho^\star(\kappa) < 1$, such that for all $\rho \in (\rho^\star(\kappa), 1]$ and for any initial state $Q(0)$:

$$\mathbb{P}_{Q(0)}\{\liminf_{t\to\infty} \|Q(t))\| = \infty\} = 1.$$

Remark 3: The class of de-activation functions $g_i(x) = \mathrm{o}(x^{-\gamma})$ includes the random-capture scheme with $g(x) \equiv 0$, $x \geq 1$, as considered in [5]. The result in Theorem 2 thus disproves the conjecture that the random-capture scheme is throughput-optimal in arbitrary topologies.

V. Simulation experiments

We now discuss the simulation experiments that we have conducted to corroborate the analytical results. Consider the network analyzed in the previous section as depicted in Figure 1(a). In the simulation experiments, the relative traffic intensities are assumed to be $\kappa = (0.4, 0.4, 0.4, 0.4, 0.2, 0.2)$, with a normalized load of $\rho = 0.97$. At each node, the initial queue size is $Q_i(0) = 500$, the activation function is $f_i(x) \equiv 1$, $x \geq 1$, and the de-activation function is $g_i(x) = x^{-\gamma}$, where we set $\gamma = 2$.

Figure 2(a) plots the evolution of the queue sizes at the various nodes over time, and shows that once a node starts transmitting, it will continue to do so until the backlogs of all nodes in its component have largely been cleared. This characteristic, and the associated oscillations in the queues, are consistent with the piecewise linear (and random oscillatory) properties of fluid limits as discussed in Section III.

Although Figure 2(a) suggests an upward trend in the overall queue lengths, the fluctuations make it hard to discern a clear picture. Figure 2(b) therefore plots the evolution of the node-average queue size over time, and reveals a distinct growth pattern. Evidently, it is difficult to make any conclusive statements concerning stability/instability based on simulation results alone. However, the saw-tooth type growth pattern in

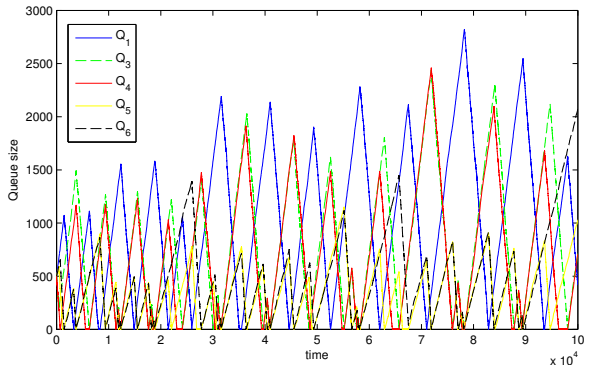

(a) Queue sizes at the various nodes as function of time.

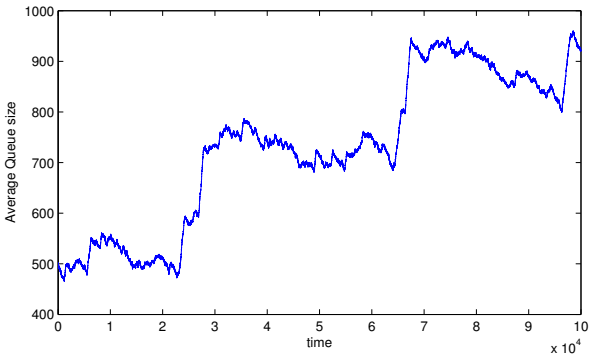

(b) Node-average queue size as function of time.

Fig. 2. Simulation of the network of Figure 1(a).

Figure 2(b) demonstrates strong signs of instability, and corroborates the qualitative growth behavior exhibited by the fluid limit as described in Section III. Indeed, careful inspection of the two figures confirms that the large increments in the node-average queue size occur immediately after the activity process leaves M_4, exactly as described by the fluid limit. We further observe that in between these periods, the node-average queue size tends to follow a slightly downward trend, consistent with the negative drift of rate $(\rho - 1)/3$ in the fluid limit.

VI. Conclusions

We have used fluid limit techniques to show that aggressive backlog-based random-access algorithms do not confer universal stability. For the sake of transparency, we focused on a specific six-node topology with super-linear activity functions. Similar instability issues can however arise in a broad class of interference graphs which contain an independent set that intersects with two maximal independent sets and is disjoint from a third one. The proof arguments further suggest that instability can in fact occur for any activity factor that grows as a positive power $1/K$ of the backlog for network sizes of order K, indicating that the growth conditions for maximum stability in Ghaderi & Srikant [7] are sharp in a certain sense.

In order to demonstrate instability in these more general scenarios, similar fluid limit approaches might be used. The framework of Meyn [16] however hinges on instability of the fluid limit *for any initial state*. Handling arbitrary initial states for general activity functions and topologies is more involved than in the specific network considered here. An alternative option would be to extend the methodology and develop a proof apparatus where it suffices to show instability of the fluid limit for one particular initial state.

References

[1] N. Bouman, S.C. Borst, J.S.H. van Leeuwaarden, A. Proutière (2011). Backlog-based random access in wireless networks: fluid limits and delay issues. In: *Proc. ITC 23*, 39–46.

[2] J.G. Dai (1995). On positive Harris recurrence of multiclass queueing networks: A unified approach via fluid limit models. *Ann. Appl. Prob.* **5**, 49–77.

[3] J.G. Dai (1996). A fluid limit model criterion for instability of multiclass queueing networks. *Ann. Appl. Prob.* **6**, 751–757.

[4] J.G. Dai, S.P. Meyn (1995). Stability and convergence of moments for multiclass queueing networks via fluid limit models. *IEEE Trans. Aut. Control* **40 (11)**, 1889–1904.

[5] M. Feuillet, A. Proutière, Ph. Robert (2010). Random capture algorithms: fluid limits and stability. In: *Proc. ITA Workshop*.

[6] J. Ghaderi, S.C. Borst, P.A. Whiting (2011). Backlog-based random-access algorithms: fluid limits and stability issues. *Technical Report*, available online at http://www.ifp.illinois.edu/~jghaderi/fl.pdf

[7] J. Ghaderi, R. Srikant (2010). On the design of efficient CSMA algorithms for wireless networks. In: *Proc. CDC 2010.*

[8] L. Jiang, M. Leconte, J. Ni, R. Srikant, J. Walrand (2011). Fast mixing of parallel Glauber dynamics and low-delay CSMA scheduling. In: *Proc. Infocom 2010 Mini-Conf.*

[9] L. Jiang, D. Shah, J. Shin, J. Walrand (2010). Distributed random access algorithm: scheduling and congestion control. *IEEE Trans. Inform. Theory* **56 (12)**, 6182–6207.

[10] L. Jiang, J. Walrand (2008). A distributed CSMA algorithm for throughput and utility maximization in wireless networks. In: *Proc. Allerton 2008.*

[11] L. Jiang, J. Walrand (2010). A distributed CSMA algorithm for throughput and utility maximization in wireless networks. *IEEE/ACM Trans. Netw.* **18 (3)**, 960–972.

[12] J. Liu, Y. Yi, A. Proutière, M. Chiang, H.V. Poor (2008). Maximizing utility via random access without message passing. Tech. Rep. MSR-TR-2008-128, Microsoft Research.

[13] M. Lotfinezhad, P. Marbach (2010). Delay performance of CSMA policies in multihop wireless networks: A new perspective. In: *Proc. ITA Workshop*.

[14] M. Lotfinezhad, P. Marbach (2011). Throughput-optimal random access with order-optimal delay. In: *Proc. Infocom 2011.*

[15] P. Marbach, A. Eryilmaz (2008). A backlog-based CSMA mechanism to achieve fairness and throughput-optimality in multihop wireless networks. In: *Proc. Allerton 2008.*

[16] S.P. Meyn (1995). Transience of multiclass queueing networks via fluid limit models. *Ann. Appl. Prob.* **5**, 946–957.

[17] J. Ni, B. Tan, R. Srikant (2010). Q-CSMA: queue-length based CSMA/CA algorithms for achieving maximum throughput and low delay in wireless networks. In: *Proc. Infocom 2010 Mini-Conf.*

[18] S. Rajagopalan, D. Shah, J. Shin (2009). Network adiabatic theorem: an efficient randomized protocol for content resolution. In: *Proc. ACM SIGMETRICS/Performance 2009.*

[19] D. Shah, J. Shin (2010). Delay-optimal queue-based CSMA. In: *Proc. ACM SIGMETRICS 2010.*

[20] D. Shah, J. Shin, P. Tetali (2011). Medium access using queues. In: *Proc. FOCS 2011.*

[21] D. Shah, D.N.C. Tse, J.N. Tsitsiklis (2011). Hardness of low delay network scheduling. *IEEE Trans. Inf. Theory*, to appear.

[22] V. Subramanian, M. Alanyali (2011). Delay performance of CSMA in networks with bounded degree conflict graphs. In: *Proc. ISIT 2011.*